

INSTRUMENTATION

Fast Count-Dependent Digital Filtering of Nuclear Medicine Images: Concise Communication

Michael A. King, Paul W. Doherty, Ronald B. Schwinger, David A. Jacobs, Robert E. Kidder, and Tom R. Miller

The University of Massachusetts Medical Center, Worcester, Massachusetts, and Washington University School of Medicine, St. Louis, Missouri

The formulation of an "optimal" filter for improving the quality of digitally recorded nuclear medicine images is reported in this paper. The method forms a Metz filter for each image based upon the total number of counts in the image, which in turn determines the average noise level. The parameters of the filter were optimized for a set of simulated images using the minimization of the mean-square error as the criterion. The speed of the image formation results from the use of an array processor. In a study of localization receiver operating characteristics (LROC) using the Alderson liver phantom, a significant improvement in tumor localization was found in images filtered with this technique, compared with the original digital images and those filtered by the nine-point binomial smoothing algorithm. The technique has been found useful for the filtering of static and dynamic studies as well as the two-dimensional pre-reconstruction filtering of images from single photon emission computerized tomography.

J Nucl Med 24: 1039-1045, 1983

Image quality in nuclear medicine is limited physically by the spatial resolution of imaging systems and the random noise inherent in the radioactive decay process. One way to improve image quality is through the computer processing of digitally recorded images. A number of different digital filtering methods have been formulated in an attempt to produce optimum restoration of the inherent image quality and suppression of noise (1-3). The method proposed here forms a filter for each image to be processed based upon the total number of counts in the image, since this determines the noise level in the frequency domain (4). The filter is truly "optimal" in the sense of minimum mean-square error only for the set of images for which it was derived but, as will be shown, it has been found useful for a number of different applications. The speed of the filtering results from its

implementation on a host computer* with an array processor†.

THEORY

Under the assumptions of linearity and shift invariance, digital imaging can be modeled mathematically in the spatial-frequency domain as (5-7):

$$G(u,v) = \text{MTF}(u,v) \cdot F(u,v) + N(u,v), \quad (1)$$

where capital letters are used to indicate the Fourier transform (FT) of the spatial-domain term, G is the FT of the image, MTF is the modulation transfer function, F is the FT of the undistorted object, N is the FT of the noise, and u and v are spatial frequencies. Ideally one would like the image to be a "true" copy of the object, instead of the blurred and noisy copy that is obtained. This can be done theoretically by solving Eq. (1) for the FT of the object and inverse-transforming the result. A least-squares solution of Eq. (1) results in an estimate of the FT of the object (\hat{F}) given by (5,6):

Received Mar. 22, 1983; revision accepted June 13, 1983.

For reprints contact: Michael A. King, PhD, Dept. of Nuclear Medicine, The University of Massachusetts Medical Center, Worcester, MA 01605.

$$\hat{F}(u,v) = \text{MTF}^{-1}(u,v) \cdot G(u,v), \quad (2)$$

which is known as the inverse filter, or the process of deconvolution. The problem is that this solution is ill-conditioned, which means that a trivial perturbation in G (such as the noise) can cause nontrivial perturbations in \hat{F} . Thus in the presence of noise there is no unique solution but rather an infinite family of possible solutions (5). The goal of image processing is to pick the "best" restored image out of this family. This is usually done by using some rational mathematical criterion to select the "best" filter.

The approach used in this study was to use the Metz filter (8,9) as a count-dependent approximation to the inverse filter. The Metz filter is defined as:

$$M(u,v) = \text{MTF}(u,v)^{-1} \cdot [1 - \{1 - \text{MTF}(u,v)\}^X], \quad (3)$$

where X is the factor (not necessarily an integer) that controls the extent to which the inverse filter is followed before the filter switches to noise suppression. That is, the filter is made up of the product of the inverse filter [first term after equal sign in Eq. (3)], and a low-pass filter (second term), and the magnitude of X determines when the low-pass filter begins to dominate.

The reasons for making X a function of the total image count is illustrated in Fig. 1, which shows normalized plots of the logarithms to the base 10 of the two-dimensional power spectra, averaged over annuli in frequency space, of three different total-count acquisitions of the Alderson Organ Scanning Phantom[†]. The average magnitude of the noise power spectrum is equal to the total image count (4). Thus, as shown in Fig. 1, as the total image count increases, the object spectrum can be distinguished at higher spatial frequencies from the flat power spectrum of the Poisson noise. That is, with increasing total image count, the object frequencies can be recovered from the noise at higher spatial frequencies without the amplification of noise-dominated terms. This means that, as the total count acquired increases, it is desirable to move the cutoff between resolution recovery (following the inverse filter) and noise suppression (following the low-pass filter) to higher spatial frequencies. Making the parameter X of the Metz filter count-dependent accomplishes this. An "optimal" relationship between X and the total count was obtained by the following methods.

METHODS

The mathematical criterion for "optimality" used in this study was that of the minimization of the mean-square error (MSE) between the filtered image and the object (5,6). The MSE is defined as:

$$\text{MSE} = \sum \sum (\hat{M}_{ij} - M_{ij})^2, \quad (4)$$

where M_{ij} is the "true" value of the pixel ij in the object

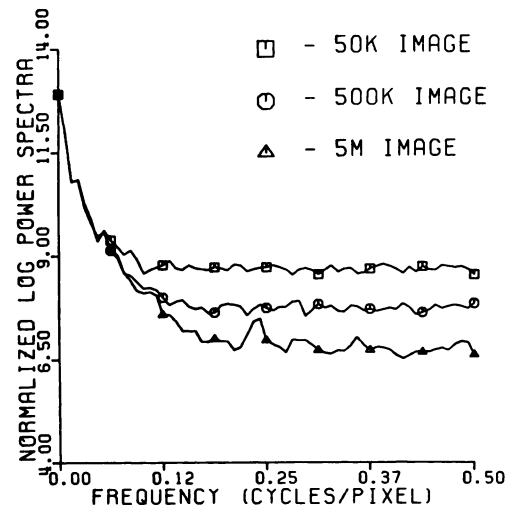


FIG. 1. Plot of \log_{10} of two-dimensional power spectra, averaged over annuli in frequency space, of Alderson Organ Scanning Phantom, acquired with total counts of 50,000, 500,000, or 5,000,000.

distribution, and \hat{M}_{ij} is its estimate in the processed image. To calculate the MSE it is necessary to know the object distribution for comparison with that of the restored image. We chose as our object a 128- by 128-pixel image of the Alderson liver phantom filled with a Tc-99m solution, and a Plexiglas "tumor" inside, with the phantom in contact with the high-resolution collimator of a standard-field-of-view camera (to maximize initial resolution). We collected for a total of 200 million counts, to minimize the noise in the image. This image was then scaled to maximum counts of 50, 100, 200, or 500 per pixel, then used as the object in Eq. (4). The images to be restored were obtained by blurring the above "object" images by the modulation transfer function (MTF) of the camera at 7.5 cm displacement from the collimator (average depth of liver in anterior view of abdomen of phantom) and then using a random-number generator to add count-dependent Poisson noise (10).

This resulted in realistically simulated liver object/image pairs, which were used to determine X according to the minimum MSE for each count level and each of two different forms for the MTF. The first form for MTF was that of the actual MTF used in blurring the

TABLE 1. VALUES OF X THAT MINIMIZED MEAN-SQUARE ERROR

Total number of counts	True MTF	Generalize MTF
154,912	2.19	3.98
311,968	2.78	4.93
626,041	3.36	5.38
1,547,160	4.11	6.56

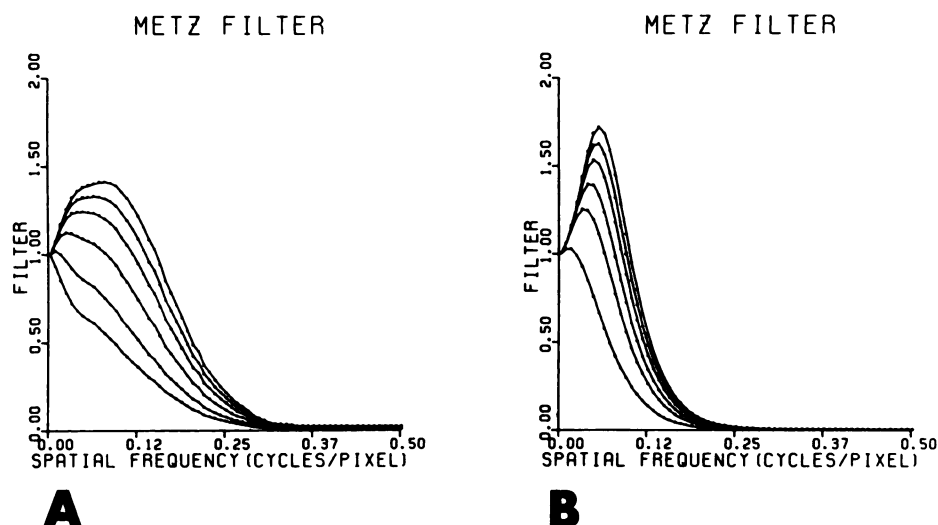


FIG. 2. Plot of optimized count-dependent Metz filter for total counts of 16,000, 64,000, 160,000; 400,000, 800,000, and 1,600,000 from the lowest to highest curves, respectively. (A) True MTF. (B) Generalized exponential model of MTF.

image. The second form was that of a generalized exponential:

$$MTF(u,v) = \exp [-(u^2 + v^2)P/S], \quad (5)$$

where P and S were parameters that were also determined as those that minimized the MSE.

As a test of the improved image quality provided by this technique, it was decided to determine whether it could provide improved "tumor" detection in phantom images where the truth of "tumor" presence and location were known. To do this, images from the Alderson Organ Scanning Phantom, processed by the count-dependent Metz filtering technique and the standard nine-point binomial smoothing technique (1-3), were compared for tumor detection with the original digital images. The Alderson phantom simulates the adult abdomen, allowing separate concentrations of activity to be placed

in liver and abdomen, and the placement of spherical "tumors" of various sizes in the liver. Five-hundred-thousand count, 128- by 128-pixel images of the phantom were obtained using a standard-field-of-view gamma camera with a high-resolution collimator. Twenty-five images were made of each of three "tumors" (diam 3 cm, 2 cm, and 1.5 cm) randomly located in the liver, and fifty images were made of the phantom with no "tumor." The images were coded as to the presence or absence of a "tumor," the "tumor" location, and its size. They were displayed using 256 shades of gray on a monitor. An observer (physician) was trained by making one practice trial run through each of the image sets. He was allowed to vary the viewing distance and take as long as desired to decide on location and scoring. A score of from one (definitely negative) to five (definitely positive) was assigned to each image to indicate his level of confidence

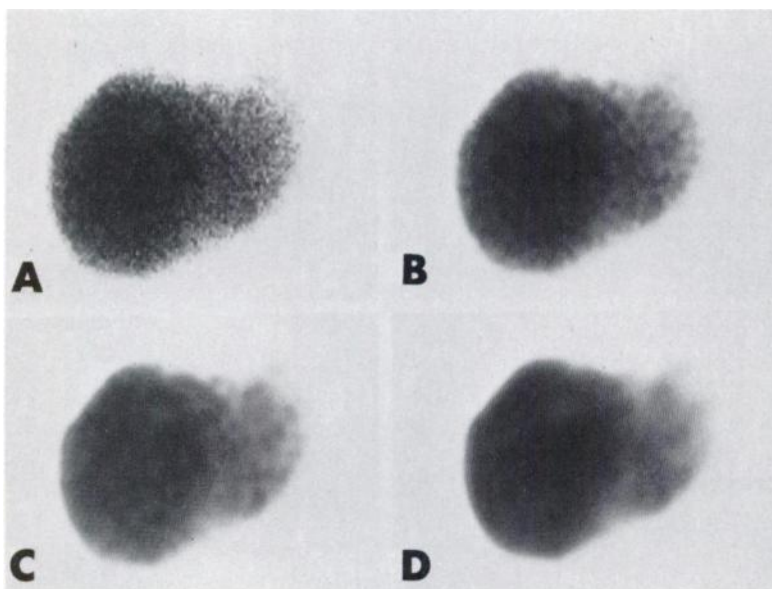


FIG. 3. Images (500 K counts) Alderson Liver Phantom with 2-cm photopenic "tumor," acquired in 128- by 128-pixel matrix. (A) Original digital image. (B) Nine-point binomial-smoothed image. (C) Image filtered by Metz filter optimized for actual MTF. (D) Image filtered by Metz filter optimized for generalized exponential model of MTF.

of the presence and location of the tumor (11). The location of the "tumor" was specified relative to a computer-generated grid overlaid on the image after scoring. The "true" location of the defect in this coordinate system was obtained from the second frame of the study, where a point source was placed behind the "tumor" to mark its location. The scores were classified as true positive with correct "tumor" location (TP_c), true positive with incorrect location (TP_i), and false positive (FP). From these, curves of the localization receiver operating characteristic (LROC) were generated for comparison among the different processing modes. LROC differs from ROC in that not only the existence but also the location of the tumor is specified (12,13).

As a statistical test of the difference between the LROC curves for the various processing techniques, the areas under the curves were compared in the following manner. First, the area under each curve and its approximate standard error were calculated (14). Then the t-test (15) was used to determine the level of significance of the differences in area.

RESULTS

Table 1 gives the values of the parameter X of the Metz filter that minimized the MSE for each of the forms used to generate the MTF. The parameters of the generalized exponential [Eq. (5)] used to obtain these data were 0.675 and 17 for P and S, respectively. These values gave the actual minimum value for the MSE at three of the four count levels. At the highest count level, values of 0.65 and 16, respectively, were determined to give the minimum MSE, but this MSE was only very slightly smaller than that obtained with P = 0.675 and S = 17. Thus the values in Table 1 for the generalized MTF were obtained using the former set of P and S in each case. The values of the MSE for the generalized

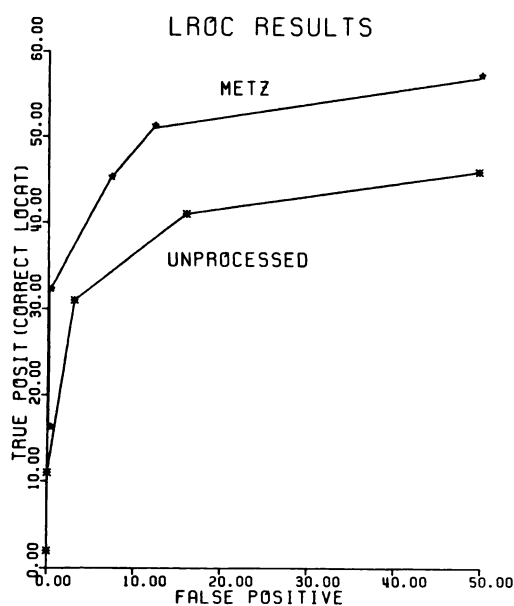


FIG. 4. Curves of localization receiver operating characteristics (LROC) for unprocessed digital images, and images processed by count-dependent Metz filter.

MTF were found to be about one half of those determined for the true MTF.

To generate the filter as a function of total image count, the data from Table 1 were fitted with a logarithmic curve, thus obtaining:

$$X = 0.834 \ln(\text{count}) - 7.774 \quad (7)$$

with a correlation coefficient of 0.999 for the true MTF, and

$$X = 1.081 \ln(\text{count}) - 8.899 \quad (8)$$

with a correlation coefficient of 0.993 for the generalized MTF. In either case, X is not allowed to fall below 1.0 during filtration of an image. Figure 2 shows the resulting filters as a function of total image counts from

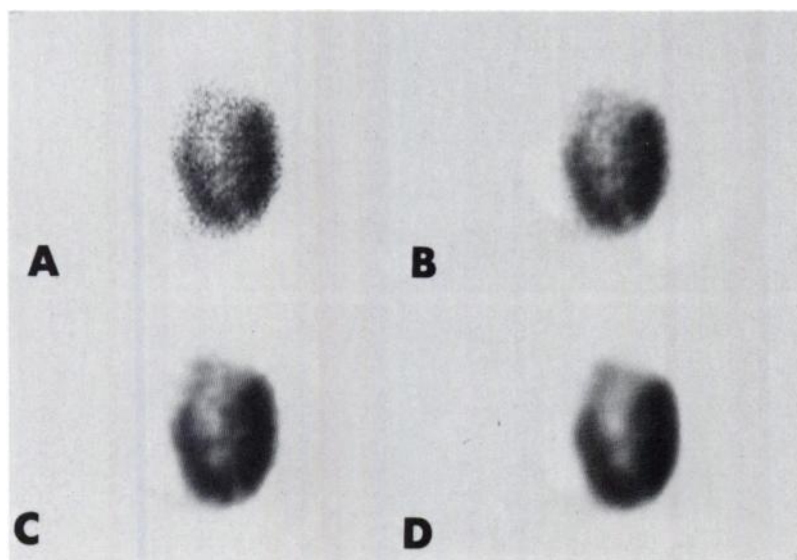


FIG. 5. LAO thallium cardiac images, 600,000 counts, 128 X 128 matrix. (A) Original unprocessed image. (B) With nine-point binomial smoothing. (C) Image filtered by Metz filter optimized for actual MTF. (D) Image filtered by Metz filter optimized for generalized exponential model of MTF.

16,000 to 1,600,000. Notice that as the total image count increases, the filters do follow the "inverse" filter to higher frequencies, as was shown to be desirable in Fig. 1. Figure 3 shows an original unprocessed image of the Alderson phantom, and the images as processed by nine-point binomial smoothing and by each of the forms of the Metz count-dependent filter. Notice that the generalized MTF produces the best resolution recovery and noise suppression as it yielded a smaller value for the MSE. For this reason only this form was used in the LROC studies.

The results of the LROC study are given in Table 2 and shown in Fig. 4. The data for nine-point smoothing are not plotted in Fig. 4 since they are very similar to the data for the unprocessed images (Table 2). By the t-test a significant ($p < 0.05$) improvement in "tumor" detection occurred with count-dependent Metz filtering when compared with the unprocessed or nine-point-smoothed digital images, but no significant difference was observed between the latter two methods.

DISCUSSION

The processing of 128- by 128-pixel images with the Metz count-dependent filter of this study takes 12 sec, a speed attained through the use of an array processor. Without it, it takes 104 sec to do the same processing with floating-point hardware, and 410 sec using our host system alone. The speed of the array processor is such that Metz count-dependent spatial filtering of 64- by 64-pixel images followed by a binomial temporal filtering can be carried out at a rate of three frames per second.

A small but significant improvement was found in the LROC evaluation of tumor detection by this processing method. Perhaps a better index of the usefulness of the

Processing method	Score	TP(CL)*	TP(IL)†	FP‡	Area (s.e.)§
Unprocessed	5	2	0	0	0.54 (0.05)
	≥4	11	0	0	
	≥3	31	1	3	
	≥2	41	8	16	
	≥1	46	29	50	
Nine-point smooth	5	1	0	0	0.51 (0.05)
	≥4	9	0	0	
	≥3	32	2	2	
	≥2	38	11	20	
	≥1	44	31	50	
Metz	5	16	0	0	0.68 (0.05)
	≥4	32	0	0	
	≥3	45	7	7	
	≥2	51	10	12	
	≥1	57	18	50	

* True positive (correct location).
† True positive (incorrect location).
‡ False positive.
§ Area under the curve and its standard error.

method is the clearer images that result. This allows for improved delineation of structure as well as detection.

Similar LROC results were observed with a nonstationary frequency domain version of this filtering technique (16), which takes about six times as long. For this reason we are now using clinically only the stationary method presented in this paper.

The Metz filters were derived and are plotted in Fig. 2 for 128- by 128-pixel studies. To filter 64- by 64-pixel studies the same form of the filters were used, but the extent of their frequency domain was limited to one half

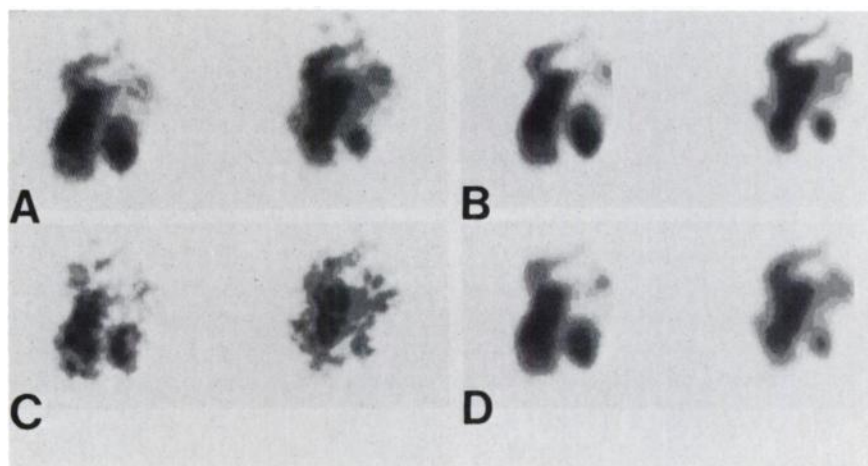


FIG. 6. Comparison of end-diastolic and end-systolic frames from gated blood-pool studies acquired in 64- by 64-pixel matrices. (A) High-count acquisition (320,000 counts per frame) filtered by nine-point smoothing. (B) High-count acquisition filtered by count-dependent Metz filter. (C) Low-count acquisition (40,000 counts per frame) filtered by nine-point smoothing. (D) Low-count acquisition filtered by count-dependent Metz filter.

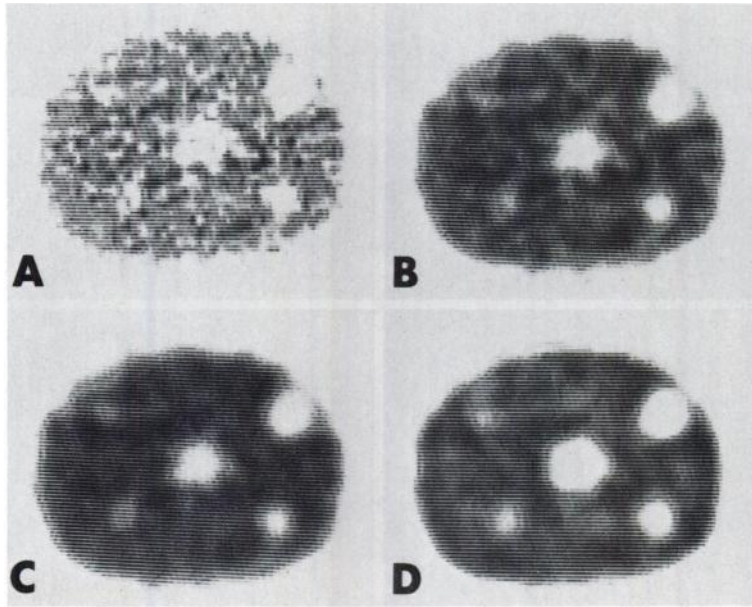


FIG. 7. Reconstructions of slice through the body of Alderson Organ Scanning Phantom with photopenic "tumors" 5, 4, 3, 2, and 1.5 cm in diam and an average of 110,000 counts per 64- by 64-pixel frame in acquired data. (A) Ramp filtered. (B) Ramp filtered with nine-point binomial smoothing after reconstruction. (C) Soft Shepp-Logan preprocessing filter (cutoff frequency was equal to two thirds the Nyquist frequency). (D) Two-dimensionally Metz-filtered before reconstruction with ramp filter.

that used for 128- by 128-pixel matrices. This was done because, by the sampling theorem, decreasing the acquisition matrix size from 128 to 64 just halves the extent of the frequency domain of the image along either axis (17). No account of the altered noise level per pixel with a change in the size of the matrix was taken in forming the filter. This is because the level of the noise power spectrum—and hence when the filter must be rolled off—is dependent only upon the total image count (4,17). This was verified by comparing the power spectra of images of phantoms collected for the same total counts as 64- by 64- and 128- by 128-pixel studies.

Although the parameters of this filter are "optimal," in the minimum-MSE sense, only for the set of images from which they were derived, they have been found quite useful in a number of applications other than the liver/spleen studies for which the Alderson phantom is a good approximation. We have used the count-dependent Metz filter to process static thallium images (Fig. 5), dynamic flow studies, and gated blood-pool studies (18). The usefulness of the count-dependent nature of the filter is illustrated in Fig. 6, where the end-diastolic and end-systolic frames of gated blood-pool studies having high counts (acquisition time 8 min), and low counts (acquisition time 1 min) are shown filtered by the nine-point binomial smoothing technique, and with the count-dependent Metz filter. Notice the marked improvement in image quality with Metz filtering, especially in the case of the low-count study. We have found this method useful for producing enhancement in high-count rest studies, and for smoothing low-count exercise studies (18).

Another application to which we have applied the count-dependent Metz filter is in the two-dimensional prereconstruction filtering of single photon emission computerized tomographic (SPECT) acquisition frames.

This technique takes advantage of the data on either side of the plane to be reconstructed to reduce the random fluctuations in the data to be back-projected. By including a deconvolutional component in the filter, the contamination of data in one plane by those from adjacent planes is minimized. The result is that higher-quality projection data are passed to the back-projection routine, resulting in better SPECT images in terms of noise level and image contrast. This noise reduction is demonstrated in Fig. 7, which shows four different filtering techniques applied to processing an emission tomographic slice through the Alderson Organ Scanning Phantom, filled with a Tc-99m solution and with five Plexiglas spheres (diam. 5.0, 4.0, 3.0, 2.0, and 1.5 cm) centered at this level. The image contrast (19) of each of these five spheres for each of the four filtering techniques was measured, and it was observed that prereconstruction filtering of the data with the Metz count-dependent filter either enhanced or maintained the image contrast of the spheres compared with their contrast obtained with the ramp filter, while reducing the noise level in the reconstructed image. The other two filtering methods of Fig. 7 both resulted in a decrease in image contrast compared with that obtained with the ramp filter. We have found the count-dependent nature of our implementation of the Metz filter to be of particular value in prefiltering thallium SPECT studies.

We note that use of the generalized exponential model of the MTF produced superior results both visually and quantitatively in terms of the minimization of the MSE when compared with use of the "true" MTF. For this reason it is probably better to think of our proposed method of Metz filtering as an enhancement technique rather than a restoration technique. This is especially true since we have found this filter useful for a number of different cameras, collimators, and radionuclides.

FOOTNOTES

- * DEC PDP 11/34, Gamma-11 System, Digital Equipment Corporation, Marlboro, MA.
 † AP400, Analogic Corporation, Wakefield, MA.
 ‡ Alderson Research Laboratories, Inc., Stamford, CT.

ACKNOWLEDGMENTS

The authors thank Karen Johnson, NMRT, for her work in acquisition of the Alderson phantom images. We also thank Linda Carreau for her assistance in the preparation of this paper. The investigation was aided by a grant from the American Cancer Society, Massachusetts Division, Inc.

REFERENCES

1. PIZER SM, TODD-POKROPEK AE: Improvement of scintigrams by computer processing. *Semin Nucl Med* 8:125-146, 1978
2. TODD-POKROPEK A: Image processing in nuclear medicine. *IEEE Trans Nucl Sci* 27:1080-1094, 1980
3. TODD-POKROPEK A, DiPAOLA R: The use of computers for image processing in nuclear medicine. *IEEE Trans Nucl Sci* 29:1299-1309, 1982
4. KING MA, DOHERTY PW, SCHWINGER RB, et al: A Wiener filter for nuclear medicine images. *Med Phys* (in press)
5. ANDREWS HC, HUNT BR: *Digital Image Restoration*. Prentice-Hall, Inc., Englewood Cliffs, 1977, pp 113-186
6. PRATT WK: *Digital Image Processing*. Wiley, New York, 1978, pp 345-425
7. CASTLEMAN KR: *Digital Image Processing*. Prentice-Hall, Inc, Englewood Cliffs, 1979, pp 139-249
8. METZ CE: A mathematical investigation of radioisotope scan image processing. Ph.D. Thesis, University of Pennsylvania, 1969
9. METZ CE, BECK RN: Quantitative effects of stationary linear image processing on noise and resolution of structure in radionuclide images. *J Nucl Med* 15:164-170, 1974
10. LO CM: Estimation of image signals with Poisson noise. Ph.D. Thesis, University of Southern California, 1979
11. METZ CE: Basis principles of ROC analysis. *Semin Nucl Med* 8:283-298, 1978
12. STARR SJ, METZ CE, LUSTED LB, et al: Visual detection and localization of radiographic images. *Radiology* 116: 533-538, 1975
13. HOUSTON AS, MACLEAD MA: An intercomparison of computer assisted image processing and display methods in liver scintigraphy. *Phys Mol Biol* 24:559-570, 1979
14. HANLEY JA, MCNEIL BJ: The meaning and use of the area under a receiver operating characteristics (ROC) curve. *Radiology* 143:29-36, 1982
15. SNEDECOR GW, COCHRAN WG: *Statistical Methods*. Sixth Edition, The Iowa State University Press, Ames, 1967, pp 91-109
16. KING MA, MILLER TR, JACOBS DA, et al: Nonstationary image processing in the frequency domain. In *Digital Imaging: Clinical Advances in Nuclear Medicine*. New York, Society of Nuclear Medicine, 1982, pp 127-141
17. KING MA, DOHERTY PW, SCHWINGER RB: Digital image filtering of nuclear medicine images. In *An Update in the Physics of Nuclear Medicine*. New York, Amer Assoc Phys Med (in press)
18. KING MA, DOHERTY PW: Cardiac image processing using an array processor. In *Digital Imaging: Clinical Advances in Nuclear Medicine*. New York, Society of Nuclear Medicine, 1982, pp 153-163
19. JASZCZAK RJ, WHITEHEAD FR, LIM CB, et al: Lesion detection with single-photon emission computed tomography (SPECT) compared with conventional imaging. *J Nucl Med* 23:97-102, 1982

**The Society of Nuclear Medicine
31st Annual Meeting**

June 5-8, 1984

Los Angeles, California

**Call for Scientific Exhibits
"One Picture is Worth a Thousand Words"**

The Scientific Exhibits Subcommittee welcomes the display of scientific exhibits at the 31st Annual Meeting in Los Angeles, CA, June 5-8, 1984. A visual discipline like nuclear medicine is particularly suited for information exchange via an exhibit format which allows the viewer good time to study, criticize, and assimilate the material; exhibits can also supplement a presented paper and provide an alternative route for the author to get his message across. Exhibits may be large or small, free standing, displayed on a posterboard, or illuminated by a viewbox, but must conform to minimal standards.

Scientific awards, based on scientific merit, originality, appearance, and other criteria will be presented in several categories this year. Abstracts selected for presentation as scientific exhibits will be published in a separate brochure that will be distributed to all those who attend the meeting.

The official abstract form may be obtained from the November 1983 JNM or by calling or writing:

Society of Nuclear Medicine
 Att: Abstracts
 475 Park Avenue South
 New York, NY 10016
 Tel: (212)889-0717

Abstracts must be submitted on the official form and received (not postmarked) by no later than Thursday, February 23, 1984.